

The role and proteomic analysis of ethylene in hydrogen gas-induced adventitious rooting development in cucumber (*Cucumis sativus* L.) explants

Dengjing Huang¹, Biting Bian¹, Meiling Zhang², Chunlei Wang¹, Changxia Li¹, Weibiao Liao^{Corresp. 1}

¹ College of Horticulture, Gansu Agricultural University, Lanzhou, PR China, Lanzhou, China

² College of Science, Gansu Agricultural University, Lanzhou, China

Corresponding Author: Weibiao Liao
Email address: liaowb@gsau.edu.cn

Previous studies have shown that both hydrogen gas (H₂) and ethylene (ETH) play positive roles in plant adventitious rooting. However, the relationship between H₂ and ETH during this process has not been explored and remains insufficiently understood. In this study, cucumber (*Cucumis sativus* L.) was used to explore the proteomic changes in ETH-H₂-induced rooting. Our results show that hydrogen-rich water (HRW) and ethylene-releasing compound (ethephon) at proper concentrations promote adventitious rooting, with maximal biological responses occurring at 50% HRW or 0.5 μM ethephon. ETH inhibitors aminoethoxyvinylglycine (AVG) and AgNO₃ cause partial inhibition of adventitious rooting induced by H₂, suggesting that ETH might be involved in H₂-induced adventitious rooting. According to two-dimensional electrophoresis (2-DE) and mass spectrometric analyses, compared with the control, 9 proteins were up-regulated while 15 proteins were down-regulated in HRW treatment; 4 proteins were up-regulated while 10 proteins were down-regulated in ethephon treatment; and 1 protein was up-regulated while 9 proteins were down-regulated in HRW+AVG treatment. Six of these differentially accumulated proteins were further analyzed, including photosynthesis-related proteins [ribulose-1,5-bisphosphate carboxylase subunit (Rubisco), sedoheptulose-1,7-bisphosphatase (SBPase), oxygen-evolving enhancer protein (OEE1)], amino and metabolism-related protein [threonine dehydratase (TDH)], stress response-related protein [cytosolic ascorbate peroxidase (CAPX)], and folding, modification and degradation-related protein [protein disulfide-isomerase (PDI)]. Moreover, the results of real-time PCR about the mRNA levels of these genes in various treatments were consistent with the 2-DE results. Therefore, ETH may be the downstream signaling molecule during H₂-induced adventitious rooting and proteins Rubisco, SBPase, OEE1, TDH, CAPX and PDI may play important roles during the process.

The role and proteomic analysis of ethylene in hydrogen gas-induced adventitious rooting development in cucumber (*Cucumis sativus* L.) explants

Dengjing Huang¹, Biting Bian¹, Meiling Zhang ², Chunlei Wang¹, Changxia Li¹, Weibiao Liao¹

¹College of Horticulture, Gansu Agricultural University, Lanzhou, PR China

²College of Science, Gansu Agricultural University, Lanzhou, PR China

Corresponding author:

Weibiao Liao

Mailing address:

College of Horticulture, Gansu Agricultural University, Anning District, Lanzhou, China

E-mail address: liaowb@gsau.edu.cn

Abstract

Previous studies have shown that both hydrogen gas (H₂) and ethylene (ETH) play positive roles in plant adventitious rooting. However, the relationship between H₂ and ETH during this process has not been explored and remains insufficiently understood. In this study, cucumber (*Cucumis sativus* L.) was used to explore the proteomic changes in ETH-H₂-induced rooting. Our results show that hydrogen-rich water (HRW) and ethylene-releasing compound (ethephon) at proper concentrations promote adventitious rooting, with maximal biological responses occurring at 50% HRW or 0.5 μM ethephon. ETH inhibitors aminoethoxyvinylglycine (AVG) and AgNO₃ cause partial inhibition of adventitious rooting induced by H₂, suggesting that ETH might be involved in H₂-induced adventitious rooting. According to two-dimensional electrophoresis (2-DE) and mass spectrometric analyses, compared with the control, 9 proteins were up-regulated while 15 proteins were down-regulated in HRW treatment; 4 proteins were up-regulated while 10 proteins were down-regulated in ethephon treatment; and 1 protein was up-regulated while 9 proteins were down-regulated in HRW+AVG treatment. Six of these differentially accumulated proteins were further analyzed, including photosynthesis-related proteins [ribulose-1,5-bisphosphate carboxylase subunit (Rubisco), sedoheptulose-1,7-bisphosphatase (SBPase), oxygen-evolving enhancer protein (OEE1)], amino and metabolism-related protein [threonine dehydratase (TDH)], stress response-related protein [cytosolic ascorbate peroxidase (CAPX)], and folding, modification and degradation-related protein [protein disulfide-isomerase (PDI)]. Moreover, the results of real-time PCR about the mRNA levels of these genes in various treatments were consistent with the 2-DE results. Therefore, ETH may be the downstream signaling molecule during H₂-induced adventitious rooting and proteins Rubisco, SBPase, OEE1, TDH, CAPX and PDI may play important roles during the process.

Keywords: Cucumber, Adventitious root formation, Hydrogen gas, Ethylene, Proteomics

Introduction

Adventitious roots are formed from non-root tissue such as leaves, stems and hypocotyls. Adventitious roots usually increase the area of roots, heightening their abilities to absorb nutrients and support plants. Additionally, adventitious roots play an important role in promoting the vegetative propagation of fine varieties and the agriculture and forestry industries. Thus, exploring the mechanism of adventitious root formation is both necessary and meaningful. The roles of signal molecules in adventitious root development have recently become a hot topic of research. Some signal molecules including auxin (Bai et al. 2012), ethylene (Pan et al. 2002), carbon monoxide (CO; Xuan et al. 2008), nitric oxide (NO), hydrogen peroxide (H₂O₂), Ca²⁺ ions, calmodulin (Liao et al. 2012), hydrogen sulfide (H₂S; Lin et al. 2012), hydrogen (H₂; Lin et al. 2014) and methane (Cui et al. 2015) have been associated with the initiation and development of adventitious roots. More studies about signal transduction will help us understand the

mechanisms involved in adventitious rooting.

Despite its simple two-carbon structure, ethylene (ETH) plays an important role in regulating plant growth and development. ETH may induce diverse effects throughout the plant life cycle, including seed germination, flower senescence and fruit ripening (Khan et al. 2017). ETH is also involved in the plant's defense reactions against pathogens or elicitor attacks, and in its responses to abiotic stresses such as wounding, hypoxia, chilling, freezing and flooding (Khan et al. 2017), indicating that ETH might be a regulator of plant growth, development and stress responses.

Since it was firstly discovered that ethylene stimulates adventitious root formation, there have been a great number of studies on the topic. Riov and Yang (1989) investigated the role of ETH in adventitious root formation in auxin-induced cuttings of *Vigna radiata* (L.) and found that ETH increased the number of adventitious roots while aminoethoxyvinylglycine (AVG, a kind of ETH inhibitor) significantly inhibited rooting. Pitts et al. (1998) used the mutations of ETH and auxin to prove that auxin and ETH are required for normal root hair elongation. Clark et al. (1999) found that aboveground adventitious roots were produced in few ETH-insensitive never-ripe tomato plants and ETH-insensitive transgenic petunia plants compared to wild type plants, and proved the positive role of ETH in adventitious root formation. Similar results were obtained from sunflower cuttings (Liu et al. 1990), mung bean hypocotyl cuttings (Pan et al. 2002), *Panax ginseng* C.A. Meyer (Bae et al. 2006), and globe artichoke seedlings (Shinohara et al. 2016). However, some researchers have indicated that ETH can inhibit adventitious root formation. Biondi et al (1990) showed that in *Prunus avium* shoot cultures, the addition of ethylene precursor 1-aminocyclopropane-1-carboxylic acid (ACC) decreased the rooting percentage while AVG caused roots to form. Some years later, the studies of Ma et al. (1998) demonstrated that AgNO_3 (another kind of ETH inhibitor) and AVG increased the number of roots in apple shoots.

Hydrogen gas (H_2), the lightest gas, is a colorless, odorless, and tasteless diatomic gas in nature. Ohsawa et al. (2007) found that H_2 can be used as an effective antioxidant therapy in the partial brain of rat, and since then, the use of H_2 in the prevention and control of various diseases has been a hot topic of research (Hong et al. 2010). More recently, the physiological functions of H_2 in higher plants have also been studied. H_2 has often been shown to respond to stresses like salt stress, drought stress, heavy metal toxicity, oxidative stress and UV-A irradiation (Jin et al. 2013, Zeng et al. 2014, Su et al. 2014), and delaying fruit senescence (Hu et al. 2014) and inducing stomatal closure (Xie et al. 2014). Recently, another function of H_2 was discovered: the promotion of adventitious root occurrence. The results of Lin et al. (2014) demonstrated that 50% HRW could mimic hemin function and restore cucumber adventitious root formation by mediating the expression of auxin signaling-related and adventitious root formation-related genes. Zhu et al. (2016) has reported that HRW treatment increases the content of nitric oxide (NO) and up-regulated cell cycle activation during adventitious root formation. Moreover, Cao et al. (2017)

suggested that HRW is involved in regulating auxin-induced lateral root formation by modulating NR-dependent NO synthesis.

Based on the results of the studies summarized above, ETH and H₂ are involved in adventitious root formation. However, the precise mechanism remains unclear. In this study, we hypothesized the exists of a relationship between ETH and H₂ during adventitious rooting in cucumber (*Cucumis sativus* L.).

To prove this hypothesis, ETH inhibitors were used. Proteomic methods have been widely applied to determine genetic and cellular function at the protein level. Many plant proteomic studies using 2-DE have found differential proteins during somatic embryogenesis, seed germination, adventitious root formation, flowering transition, and stem dormancy. Proteomic analysis has also proven useful in the identification of proteins associated with a range of biotic and abiotic stress responses (Cui et al. 2015, Xu et al. 2016). Therefore, 2-DE and matrix-assisted laser desorption/ionization time-of-flight/time-of-flight (MALDI-TOFTOF) were used to compare quantitative and qualitative changes that occurred during ethylene-H₂-induced adventitious rooting in the proteome. Through the comprehensive analysis of the function and content of differential proteins under different treatments and the expression of genes related to these proteins, we speculate that ETH possibly affect the expression of some proteins and the expression of their related genes. The results provide new insights into the physiological and molecular mechanisms associated with adventitious root development.

Materials and Methods

Plant materials and treatments

Cucumber (*Cucumis sativus* L. var. ‘Xinchun 4’) seeds were purchased from Gansu Agricultural Institute (Lanzhou, China). The seeds were surface-sterilized in 5% sodium hypochlorite for 10 min and washed with water. The seeds were germinated on filter paper with distilled water in Petri dishes (15 cm-diameter, 2.5 cm-deep) and maintained at 25±1°C for 7 d with a 14-h photoperiod (photosynthetically active radiation = 200 μmol m⁻² s⁻¹). The 7-day-old seedlings with primary roots removed were used as explants and were maintained under the same temperature and photoperiod conditions for another 7 days in the presence of different media as indicated below. We described these different treatments as (I) HRW (0, 1%, 10%, 50% and 100%); (II) ethephon (0, 0.1, 0.5, 1, 10 and 50 μmol·L⁻¹); (III) AVG (aminoethoxyvinylglycine, 0, 0.1, 1, 5 and 10 μmol·L⁻¹); (IV) AgNO₃ and NaNO₃ (0, 0.1, 0.3 and 0.5 μmol·L⁻¹); and (V) 50% HRW + 0.5 μmol·L⁻¹ ethephon, 1 μmol·L⁻¹AVG, or 0.1 μmol·L⁻¹ AgNO₃. After applying treatment explants were sampled to determine root number per explants. The hypocotyls (5-mm-long segments of the hypocotyl base where the adventitious root develops) of the explants after 48 h of treatment were immediately used or frozen in liquid nitrogen for further analysis.

Preparation of hydrogen-rich water (HRW)

Purified H₂ gas (99.99 %, v/v) generated from a hydrogen gas generator (QL-300, Saikesaisi

Hydrogen Energy Co., Ltd., China) was bubbled into distilled water at a rate of 300 mL min⁻¹ for 30 min. The corresponding HRW was rapidly diluted to the required saturations (Zhu et al. 2016). The H₂ concentration analyzed by gas chromatography in freshly prepared HRW was 0.68 mM, which was defined as 100% HRW, and was maintained at a relatively constant level in 25 °C for at least 12 h.

Quantification of ethylene

ETH was detected by a gas chromatographic analyzer (SP-3420A, Beifenruili Inc., China). Five fresh cucumber explants were placed in 20 mL vials, stoppered with secure rubber caps, and containing 1 mL culture solution. These vials had the same conditions as before when the seedlings grew for 12 h. A gas sample (2.5 mL) was extracted and injected into a gas chromatograph, which was fitted with a GDX-502 column (2 m×3.2 mm) and a flame ionization detector. The temperature of the column, inlet and detector were 50, 140 and 240 °C, respectively. The flow rate of nitrogen gas, the carrier gas, was 30 mL·min⁻¹. ETH production was expressed as μL·h⁻¹·kg⁻¹FW.

Protein extraction

The trichloroacetic acid (TCA)/acetone method was used to extract the total protein (Damerval et al. 1986). Approximately 2.0 g of the sample was manually ground to a fine powder in liquid nitrogen with 0.04 g crosslinking polyvinylpyrrolidone (PVPP) and split into 6 tubes. The powder was suspended in 2 mL of acetone containing 10% w/v TCA and 0.07% v/v β-mercaptoethanol (β-ME). After precipitation at -20°C for at least 8 h or overnight, the pellet was collected by centrifuging at 12,000×g for 30 min. Then the powder was suspended in 2 mL of ice cold acetone (-20°C) containing 0.07% (v/v) β-ME at 4°C for 1 h, then centrifuged at 12,000×g for 20 min, and washed two times. The powder was then suspended in 2 mL of 80% acetone containing 0.07% (v/v) β-ME at 4°C for 30 min, centrifuged at 12,000×g for 15 min, and washed two times. The supernatant was removed and the pellets were dried in a freezer dryer. After air-drying, the powder was dissolved in a hydration solution [7 M urea, 2 M thiourea, 4% (w/v) 3-[(3-Cholamidopropyl)dimethylammonio]propanesulfonate (CHAPS), 1% (w/v) DL-Dithiothreitol (DTT)] at a normal temperature for 2 h, then centrifuged at 12,000×g for 30 min. The supernatant was the total protein. The protein content was determined calorimetrically using bovine serum albumin as a standard. Protein samples were stored at -80°C for further analysis.

2-DE and staining

Sample aliquots containing protein were applied to 17 cm pH 4–7 immobilized pH gradient (IPG) strips, and small volumes of lysis buffer were added to the sample aliquots. Isoelectric focusing was performed on a PROTEAN IEF Cell system (Bio-Rad) for a total of 76 kVh at 20°C. The voltage was set at 50 V for 14 h, 250 V for 1.5 h, 1000 V for 2.5 h, 9000 V for 5 h, and were run at 90000 V and then 500 V for a maximum of 24 h. Next, the gels were run using the PROTEAN II xi cell system (Bio-Rad) at 100 V for 1 h, followed by 250 V until the bromophenol blue nearly reached the bottom of the gel. After electrophoresis, staining was performed by placing

the gels into Coomassie brilliant blue solution for 17 h. To provide support for the cucumber proteomics, we performed system optimization of the pH IPG strips, loading quantity and separation gel concentration. The protein spots on the pH 3-10 gels show that the acidic side (pH 3-5) in the region of the protein particle distribution was less than alkaline side (pH 9-10) area, forming a longitudinal tail (*Fig. S1*). Most of the explant protein spots were focused in the pH 4-7 region. The results showed that 800 µg of loading quantity was optimal (*Fig. S2*), and 12% (w/v) gel concentration separation was the best choice to obtain the good resolving effect (*Fig. S3*). The results also showed that pH 4-7 IPG strips (17 cm, nonlinear; Bio-Rad), 800 µg loading quantity and 12% (w/v) separation gel concentration was the most suitable combination for isoelectric focusing of the explants' total protein in cucumber.

Image analysis and protein identification

The proteins in the gels were visualized by CBB-G250 staining. The gel images were obtained at a resolution of 300 dpi and then imported into PDQuest 8.0 (Bio-Rad). The protein spots were excised from CBB-stained preparative polyacrylamide gels. The MS and MS/MS data for protein identification were obtained with a MALDI-TOF/TOF instrument (Zhang et al. 2015). The database NCBI (<https://www.ncbi.nlm.nih.gov/>) were used to match and identified the protein spots. According to Gene Ontology and UniProt Protein Knowledgebase (<http://www.uniprot.org/>), the gene ontology (GO) analysis was performed on the proteins identified by mass spectrometry. The proteomic data have been uploaded to the Supplemental Files.

Total RNA extraction and real time PCR

Total RNA from each sample was isolated using a MiniBEST Plant RNA Extraction Kit (TaKaRa, Beijing, China). Total RNA was reverse-transcribed by using the PrimeScript™RT Master Mix (Perfect Real Time) according to the manufacturer's manual (Takara, Beijing, China). Quantitative real-time PCR was performed with a LightCycler 96 Real- Time PCR System (Roche, Switzerland) using SYBR® *Premix Ex Taq*™ II (TaKaRa, Beijing, China). Every PCR reaction was performed twice, with three independent replicates. The relative expression level of each gene was acquired using a comparative Ct method followed by internal control normalization. PCR was carried out in 20 µL volumes using the following amplification protocol: 10 s at 95°C, followed by 40 cycles of 15 s at 95°C, and then annealing at 60°C for 30 s. The relative quantization of gene expression was calculated and normalized to Actin. The expression change was calculated using the $2^{-\Delta\Delta Ct}$ method. The primers used for PCR analysis are listed in *Table 1*.

Results

Effects of different concentrations of HRW and ethephon on adventitious root development

To understand the effect of H₂ on adventitious root development, cucumber explants were treated with different concentrations of HRW (0, 1%, 10%, 50% and 100%). As shown in *Fig. 1*, different concentrations of HRW affected the development of adventitious roots. The cucumber explants treated with 50% and 100% HRW produced more adventitious roots than the control explants, but the root number under the 1% HRW treatment was significantly lower than that of the control. The maximum root number was observed with 50% HRW treatment (*Fig. 1*) and this was used for further study.

Different concentrations of ethephon, ETH-releasing compound, also had significant effects on the development of adventitious roots (*Fig. 2*). Lower concentrations of ethephon (0.1, 0.5, 1, and 10 $\mu\text{mol}\cdot\text{L}^{-1}$) increased adventitious root number, while the high concentration (50 $\mu\text{mol}\cdot\text{L}^{-1}$) significantly inhibited adventitious roots. The maximum inducible response was observed in 0.5 $\mu\text{mol}\cdot\text{L}^{-1}$ ethephon-treated explants (*Fig. 2*). Thus, we used 0.5 $\mu\text{mol}\cdot\text{L}^{-1}$ to further investigate the role of ethylene in rooting.

Effects of ethylene inhibitors AVG and AgNO₃ on H₂-induced adventitious root development

To further study the function of ETH in adventitious root formation, ethylene inhibitors were used. Results shown in *Fig. S4* and *Fig. S5* indicate that various concentrations of ETH synthesis inhibitors AVG and AgNO₃ have negative effects on rooting. We used 1 $\mu\text{mol}\cdot\text{L}^{-1}$ AVG and 0.1 $\mu\text{mol}\cdot\text{L}^{-1}$ AgNO₃ for further study. As seen in *Fig. 3*, explants treated with either HRW or ethephon alone showed improved adventitious rooting when compared with the control. Although explants treated with HRW plus ethephon had higher root number, they were not significantly higher than explants treated with either HRW or ethephon alone. When AVG (inhibitor of ETH synthesis) or AgNO₃ (an ETH action inhibitor) was added to the HRW, the inducing effects of ethephon on adventitious rooting were reversed (*Fig. 3*). Thus, we deduce that ETH might be involved in H₂-induced adventitious root development.

Effect of H₂ on ETH production and ETH-related genes' expression

As shown in *Fig. 4A*, the production of ETH in 50% HRW treatment was about double that of the control. Moreover, the results in *Fig. 4B* indicate that HRW treatment significantly enhances the gene expression of *CsACS3*. When compared with the control, the expression of *CsACO1* was noticeably improved by HRW. These consistent results suggested that ETH might function in the downstream of H₂-induced adventitious root formation.

Comparison of 2-DE gels and protein identification during adventitious root development

All 70 protein spots from the 2-DE gels showed statistical differences. However, due to limited genomic information about *C. sativus* in the NCBI database, only 48 differentially expressed protein spots could be identified by MALDI TOF/TOF MS/MS with a significant search score, shown in *Table 2* and *Fig. 5*. Out of the 48 differential proteins selected by analysis, 15 proteins were down-regulated while 9 (spot 203, 230, 858, 158, 975, 1116, 1132, 626 and 1140) were up-

regulated in the HRW treatment; 10 proteins were down-regulated and 4 (spot 2129, 1908, 1561, 1284) were up-regulated in the ethephon treatment; 9 proteins were down-regulated while 1 (spot 239) was up-regulated in the HRW + AVG treatment. *Table 2* shows a list of the putative names of proteins, matching species, protein score, accession number, molecular weights (MW), isoelectric point (PI), peptides count and Up/Down regulation. The results indicate that matching species listed above originated from the cucumber database, with molecular weights ranging from 9.4 to 75.3 KDa, PI of spots ranging from 4.31 to 8.6, protein scores ranging from 62 to 905, and matched peptide counts between 2 and 27.

Functional analysis of the six identified proteins

Forty-eight protein spots were identified using the annotated NCBI database, and these were designated as 41 known proteins and seven unknown proteins. Using the Gene Ontology and UniProt Protein Knowledgebase, all of the identified proteins were categorized into eight major groups (*Fig. 6*). Among these, Seventeen (17) photosynthesis-related proteins constituted the largest percentage (35.4%), followed by six energy metabolism-related proteins (12.5%), six translation and transcription-related proteins (12.5%), six protein folding, modification and degradation-related proteins (12.5%), three stress response-related proteins (6.3%), two amino acid metabolism-related proteins (4.2%), one cellular cytoskeleton-related proteins (2.1%), and seven unknown proteins (14.6%).

The differentially expressed proteins were identified using mass spectrometry and GO ontology analysis. These proteins were distributed in 3 categories: “biological process” (the largest group), “cellular component” and “molecular function” (the smallest group). As shown in *Fig. 7*, 4 categories of proteins were identified in the biological process, comparing cellular process, metabolic process, response to stimulus and single-organism process; 3 categories of proteins were identified in molecular function, comparing: catalytic activity, transporter activity and binding; and 6 categories of proteins were identified in the cellular components, including organelles, cell parts and so on.

Out of the 41 proteins with known functions, 5 proteins were up-regulated in HRW or ethephon treatment, and were down-regulated in HRW + AVG treatment. these included ribulose-1,5-bisphosphate carboxylase small subunit (Rubisco), sedoheptulose-1,7-bisphosphatase (SBPase), threonine dehydratase (TDH), cytosolic ascorbate peroxidase (CAPX), and protein disulfide-isomerase (PDI) (*Table 3*). The oxygen-evolving enhancer protein (OEE1) was down-regulated under HRW or ethephon treatment and up-regulated under HRW + AVG treatment.

Validation of the identified proteins at the mRNA level during adventitious root development

The mRNA levels of Rubisco, SBPase, TDH, CAPX and PDI genes under HRW or ethephon treatment were significantly higher than those of the control (*Fig. 8*). However, HRW + AVG treatment caused significant reduction in the expression of these genes. The mRNA levels of OEE1 increased significantly in the explants treated with HRW or ethephon, and decreased

significantly in the explants treated with HRW+AVG. The changes of the mRNA levels of 6 genes were consistent with protein levels observed in the 2-DE results.

Discussion

Since Renwick et al. (1964) first reported that H₂ could promote germination, the function of H₂ in plants has been extensively investigated. Recently, H₂ has been linked to a wide variety of physiological processes in plants, ranging from the control of developmental processes to the regulation responses to abiotic stresses (Xie et al. 2012, Hu et al. 2014, Wu et al. 2015, Chen et al. 2017). Lin et al. (2014) and Zhu et al. (2017) reported that H₂ plays positive roles in adventitious root development. In our study, suitable concentrations of exogenous H₂ significantly promoted the formation of adventitious roots in cucumber. Moreover, ETH was also found to be involved in adventitious rooting. Previous studies showed that ETH stimulated adventitious root formation in some crops including mung bean (Pan et al. 2002), sunflower (Liu et al. 1990) and marigold (Jin et al. 2017). Xu et al. (2017) revealed that ETH increased the formation of adventitious root in dose-dependent experiments. Our results suggested that exogenous ETH and 0.5 μmol·L⁻¹ ethephon significantly enhanced adventitious rooting. Evidently, both H₂ and ETH can induce adventitious rooting, but the interaction between H₂ and ETH during that process remains poorly understood. The results in this study suggest that ETH is involved in the H₂-induced adventitious rooting process and might function at the downstream of H₂.

We found that the selected ethylene inhibitors AVG and AgNO₃, caused partial inhibition of H₂-induced adventitious root development. When comparing HRW and the control in the production of ETH and the expression of two ETH-related genes, the HRW treatment was obviously higher than the control. These results suggest that ETH may be a downstream signal molecule in H₂-induced adventitious root development.

To further prove that ETH is involved in H₂-induced adventitious root formation, we used proteomic analysis, which allowed us to identify proteins whose expression was altered during adventitious rooting particularly in regard to H₂ and ETH treatments. The results of proteomic analysis showed that there were 41 differential proteins with known functions successfully identified in the adventitious root formation of cucumber. They were distributed among 3 categories. We also found 6 proteins, Rubisco, SBPase, TDH, CAPX, PDI and OEE1, to be used for further study.

It is known that Rubisco, SBPase and OEE1 proteins are related to the photosynthetic process. Rubisco is a vital enzyme associated with carbon fixation (Xu et al. 1994) and its catalytic inefficiencies often limit plant productivity (Andersson et al. 2008, Gunn et al. 2017). SBPase has been shown to increase photosynthetic capacity and plant yield and it also promotes the growth of plants at the early growth stage (Ogawa et al. 2015). Our results show that Rubisco

and SBPase expression were up-regulated under HRW or ethephon treatment, suggesting that H₂ and ETH may increase the efficiency of photosynthesis in explants by enhancing Rubisco and SBPase expression during rooting. ETH inhibitor AVG inhibited the inducing effects of HRW on Rubisco and SBPase, further indicating that ETH may play important roles in the regulation of H₂ during H₂-induced adventitious root formation.

OEE1 has been suggested to be involved in photosynthesis and PS II activities (Yabuta et al. 2008). Chen et al. (2017) reported that OEE1 protein is necessary for oxygen evolving activity and is vital to maintain the stability of photosystem II. Sugihara et al. (2000) demonstrated that the level of OEE1 increased under NaCl treatment, and similar results were obtained at the transcription level. Fatehi et al. (2012) proposed that OEE1 was up-regulated in response to salinity, although in their study, H₂ and ETH treatment down-regulated OEE1 expression. This was similar to the results of Bai et al. (2017) who reported that the protein levels of OEE1 in oat leaves decreased in response to salinity. The possible explanation for this discrepancy is that OEE1 may change under different transcription, translation or treatment.

Amino acid metabolism has been found to play an important role in plant protein synthesis, photosynthesis, and development (He et al. 2013). TDH, a key enzyme in amino acid metabolism, contribute to both carbon skeleton supply and ammonium assimilation in plants and also plays an important role in metabolic acclimation (Möckel et al. 1992). Our study suggests that H₂ up-regulated TDH expression and ETH inhibitor AVG suppress the inducing effects. Proteomic analysis showed higher levels of TDH accumulation in wild ginseng than in cultivated ginseng (Sun et al. 2016). Moreover, proteomic analysis of rice and wheat coleoptiles revealed the potential role of amino acid biosynthesis in cellular anoxia tolerance (Shingakiwells et al. 2011). Thus, H₂ may increase carbon skeleton supply and metabolic acclimation in explants by enhancing TDH expression, which promotes adventitious root development. ETH is essential during this process. CAPX plays an essential role in the antioxidant defense mechanism (Wu et al. 2014) regulates plant growth, and induces organ formation (Zhang et al. 2013). The involvement of APX in fruit ripening and senescence has been proposed (Torres et al. 2003; Giribaldi et al. 2007), and Caverzan et al. (2012) demonstrated that APX genes can regulate both plant response to stresses and plant development. Additionally, *APX* mutant plant genes showed alterations in growth, physiology and antioxidant metabolism, suggesting the function of APX in plant development. Our results also show that CAPX expression was up-regulated by HRW or ethephon treatment, suggesting that H₂ may increase the reduction of oxidative damage and increase the productivity of explants by enhancing CAPX expression. However, ETH inhibitor AVG depressed the promotive effects of HRW on CAPX. PDI, related to protein folding, modification and degradation, is a multifunctional protein in cells that assists many protein maturation processes (Wilkinson et al. 2004). It may catalyze protein thiol oxidation and restore and catalyze transformation disulfide bonds (Houston et al. 2005). PDI is also mainly associated with the protein secretory pathway in plants (Irsigler et al. 2007), and has been found to be down-regulated in rice under freezing stress (Hashimoto and Komatsu 2007) and in soybean

leaves under drought stress (Irsigler et al. 2007). In our study, PDI was up-regulated under HRW treatment and down-regulated under HRW+AVG treatment, suggesting that H₂ may increase the capacity of disulfide-bonded proteins by enhancing PDI expression. Meanwhile, ETH inhibitor AVG reverses the inducing effects of HRW on PDI, indicating that ETH may play important roles in H₂-induced CAPX and PDI expression during rooting.

Conclusion

Our results show that both H₂ and ETH play crucial roles in promoting adventitious root development. ETH might work as a downstream signaling molecule during H₂-induced rooting. Further proteomic studies show that photosynthesis-related proteins (Rubisco and SBPase), amino and metabolism-related protein (TDH), stress response-related protein (CAPX), and folding, modification and degradation-related protein (PDI) may play positive roles in the ETH-H₂-induced adventitious rooting process. Oxygen-evolving enhancer protein (OEE1) may play inhibiting roles during that process. The mechanisms underlying adventitious root development are very complex and more research will need to be carried out to fully understand adventitious rooting signaling.

Acknowledgments

We thank Dr. Yongchao Zhu from Zhejiang University for providing guidance on experimental methods. We also thank Dr. Chen Bai from Gansu Academy of Agricultural Sciences for supplying a gas chromatographic analyzer.

References

- Andersson I (2008) Catalysis and regulation in Rubisco. *J Exp Bot.* 59, 1555-1568. doi:10.1093/jxb/ern091
- Bae KH, Choi YE, Shin CG, Kim YY, Kim YS (2006) Enhanced ginsenoside productivity by combination of ethephon and methyl jasmoate in ginseng (*Panax ginseng* CA Meyer) adventitious root cultures. *Biotechnol Lett*, 28(15), 1163-1166. doi:10.1007/s10529-006-9071-1
- Bai JH, Qin Y, Liu JH, Wang YQ, Sa R, Zhang N, Jia RN (2017) Proteomic response of oat leaves to long-term salinity stress. *Environ Sci Pollut R.* 24, 3387-3399. doi:10.1007/s11356-016-8092-0
- Bai XG, Todd CD, Desikan R, Yang YP, Hu XY (2012) N-3-Oxo-Decanoyl-L-Homoserine-Lactone activates auxin-induced adventitious root formation via hydrogen peroxide- and nitric oxide-dependent cyclic GMP signaling in mung bean. *Plant Physiol.* 158, 725-736. doi: 10.1104/pp.111.185769
- Beyer EM (1976) A potent inhibitor of ethylene action in plants. *Plant Physiol.* 58, 268-271. doi: 10.1104/pp.58.3.268
- Biondi S, Diaz T, Iglesias I, Gamberini G, Bagni N (1990) Polyamines and ethylene in relation to adventitious root formation in *Prunus avium* shoot cultures. *Physiol plantarum*, 78(3), 474-483. doi:10.1111/j.1399-3054.1990.tb09066.x
- Cao Z, Duan X, Yao P, Cui W, Cheng D, Zhang J, Jin Q, Chen G, Dai T, Shen W (2017) Hydrogen gas is involved in auxin-induced lateral root formation by modulating nitric oxide synthesis. *Int J Mol Sci*, 18(10), 2084. doi:10.3390/ijms18102084
- Caverzan A, Passaia G, Rosa SB, Ribeiro CW, Lazzarotto F, Margis-Pinheiro M (2012) Plant responses to stresses: role of ascorbate peroxidase in the antioxidant protection. *Genet Mol Biol*, 35(4), 1011-1019. doi:10.1590/S1415-47572012000600016
- Chen Y, Wang M, Hu LL, Liao WB, Li CL (2017) Carbon monoxide is involved in hydrogen gas-induced adventitious root development in cucumber under simulated drought stress. *Front Plant Sci.* 8, 128. doi: 10.3389/fpls.2017.00128
- Chen Z, Zhang GY, Yang MK, Li T, Ge F, Zhao JD (2017) Lysine acetylome analysis reveals photosystem II manganese-stabilizing protein acetylation is involved in negative regulation of oxygen evolution in model cyanobacterium *synechococcus* sp. PCC 7002. *Mol Cell Proteomics.* 16, 1297-1311. doi: 10.1074/mcp.M117.067835
- Clark DG, Gubrium EK, Barrett JE, Nell TA, Klee HJ (1999) Root formation in ethylene-insensitive plants. *Plant Physiol*, 121(1), 53-60. doi:10.1104/pp.121.1.53
- Cui DZ, Wu DD, Liu J, Li DT, Xu CY, Li S, Li P, Zhang H, Liu X, Jiang C, Wang LW, Chen TT, Chen HB, Zhao L (2015) Proteomic analysis of seedling roots of two maize inbred lines that differ significantly in the salt stress response. *Plos One* 10, e0116697. doi: 10.1371/journal.pone.0116697
- Cui WT, Qi F, Zhang YH, Cao H, Zhang J, Wang R, Shen WB (2015) Methane-rich water induces cucumber adventitious rooting through heme oxygenase1/carbon monoxide and

- Ca²⁺ pathways. *Plant Cell Rep.* 34, 435-445. doi: 10.1007/s00299-014-1723-3
- Damerval C, Vienne DD, Zivy M, Thiellement H (1986) Technical improvements in two-dimensional electrophoresis increase the level of genetic variation detected in wheat-seedling proteins. *Electrophoresis* 7, 52-54. doi: 10.1002/elps.1150070108
- Fatehi F, Hosseinzadeh A, Alizadeh H, Brimavandi T, Struik PC (2012) The proteome response of salt-resistant and salt-sensitive barley genotypes to long-term salinity stress. *Mol Biol Rep.* 39, 6387-6397. doi: 10.1007/s11033-012-1460-z
- Giribaldi M, Perugini I, Sauvage FX, Schubert A (2007) Analysis of protein changes during grape berry ripening by 2-DE and MALDI-TOF. *Proteomics* 7, 3154-3170. doi: 10.1002/pmic.200600974
- Gunn LH, Valegard K, Andersson I (2017) A unique structural domain in *Methanococcoides burtonii* ribulose-1, 5-bisphosphate carboxylase/oxygenase (Rubisco) acts as a small subunit mimic. *J Biol Chem.* 292, 6838-6850. doi: 10.1074/jbc.M116.767145
- Hashimoto M, Komatsu S (2007) Proteomic analysis of rice seedlings during cold stress. *Proteomics* 7, 1293-1302. doi: 10.1002/pmic.200600921
- He Y, Dai SJ, Zhu N, Pang QY, Chen SX (2013) Integrated proteomics and metabolomics of *Arabidopsis* acclimation to gene-dosage dependent perturbation of isopropylmalate dehydrogenases. *Plos One* 8, e57118. doi: 10.1371/journal.pone.0057118
- Hong Y, Chen S, Zhang JM (2010) Hydrogen as a selective antioxidant: a review of clinical and experimental studies. *J Int Med Res.* 38, 1893-1903. doi: 10.1177/147323001003800602
- Houston NL, Fan C, Xiang JQ, Schulze JM, Jung R, Boston RS (2005) Phylogenetic analyses identify 10 classes of the protein disulfide isomerase family in plants, including single-domain protein disulfide isomerase-related proteins. *Plant Physiol.* 137, 762-778. doi: 10.2307/4629717
- Hu HL, Li PX, Wang YN, Gu RX (2014) Hydrogen-rich water delays postharvest ripening and senescence of kiwifruit. *Food Chem.* 156, 100-109. doi: 10.1016/j.foodchem.2014.01.067
- Ichikawa Y, Tamoi M, Sakuyama H, Maruta T, Ashida H (2012) Generation of transplastomic lettuce with enhanced growth and high yield. *Food Chem.* 1, 322-326. doi: 10.4161/gmcr.1.5.14706
- Irsigler AS, Costa MD, Zhang P, Reis PA, Boston RS, Fontes EP (2007) Expression profiling on soybean leaves reveals integration of ER- and osmotic-stress pathways. *BMC Genomics* 8, 431. doi: 10.1186/1471-2164-8-431
- Jin Q, Zhu K, Cui W, Xie Y, Han B, Shen WB (2013) Hydrogen gas acts as a novel bioactive molecule in enhancing plant tolerance to paraquat-induced oxidative stress via the modulation of heme oxygenase-1 signalling system. *Plant Cell Environ.* 36, 956-969. doi: 10.1111/pce.12029
- Jin X, Liao WB, Yu JH, Ren PJ, Mohammed MD, Wang M, Niu LJ, Li XP, Xu XT (2017) Nitric oxide is involved in ethylene-induced adventitious rooting in marigold (*Tagetes erecta* L.). *J Hort Sci Biotech.* 97, 620-631. doi: 10.1139/CJPS-2016-0156
- Khan NA, Khan MIR, Ferrante A, Poor P (2017) Editorial: Ethylene: A Key Regulatory Molecule in Plants. *Plant Physiol.* 8, 1728. doi: 10.3389/fpls.2017.01782

- 481 Liao WB, Zhang ML, Huang GB, Yu JH (2012) Ca²⁺ and CaM are involved in NO- and H₂O₂-
482 induced adventitious root development in marigold. *J Plant Growth Regul.* 31, 253-264. doi:
483 10.1007/s00344-011-9235-7
- 484 Lin YT, Li MY, Cui W, Lu W, Shen WB (2012) Haem oxygenase-1 is involved in hydrogen
485 sulfide-induced cucumber adventitious root formation. *J Plant Growth Regul.* 31, 519-528.
486 doi: 10.1007/s00344-012-9262-z
- 487 Lin YT, Zhang W, Qi F, Cui YT, Xie YJ, Shen WB (2014) Hydrogen-rich water regulates
488 cucumber adventitious root development in a heme oxygenase-1/carbon monoxide-
489 dependent manner. *J Plant Physiol.* 17, 11-8. doi: 10.1016/j.jplph.2013.08.009
- 490 Liu J, Mukherjee L, Reid DM (1990) Adventitious rooting in hypocotyls of sunflower
491 (*Helianthus annuus*) seedlings. III. The role of ethylene. *Physiol Plantarum*, 78(2), 268-276.
492 doi:10.1111/j.1399-3054.1990.tb02091.x
- 493 Liu JH, Mukherjee I, Reid DM (1990) Adventitious rooting in hypocotyls of sunflower
494 (*Helianthus annuus*) seedling. III. The role of ethylene. *Physiol Plantarum* 78, 268-276. doi:
495 10.1111/j.1399-3054.1990.tb02091.x
- 496 Ma JH, Yao JL, Cohen D, Morris B (1998) Ethylene inhibitors enhance in vitro root formation
497 from apple shoot cultures. *Plant Cell Rep*, 17(3), 211-214. doi:10.1007/s002990050380
- 498 Möckel B, Eggeling L, Sahm H (1992) Functional and structural analyses of threonine
499 dehydratase from *Corynebacterium glutamicum*. *J Bacteriol.* 174(24), 8065-8072. doi:
500 10.1128/jb.174.24.8065-8072.1992
- 501 Ogawa T, Tamoi M, Kimura A, Mine A, Sakuyama H, Yoshida E, Maruta T, Suzuki K, Ishikawa
502 T, Shigeoka S (2015) Enhancement of photosynthetic capacity in *Euglena gracilis* by
503 expression of cyanobacterial fructose-1,6-/sedoheptulose-1,7-bisphosphatase leads to
504 increases in biomass and wax ester production. *Biotechnol Biofuels.* 8, 1-11.
505 doi:10.1186/s13068-015-0264-5
- 506 Ohsawa I, Ishikawa M, Takahashi K, Watanabe M, Nishimaki K, Yamagata K, Katsura K,
507 Katayama Y, Asoh S, Ohta S (2007) Hydrogen acts as a therapeutic antioxidant by
508 selectively reducing cytotoxic oxygen radicals. *Nat Med.* 13, 688-694. doi: 10.1038/nm1577
- 509 Pan R, Wang JX, Tian XS (2002) Influence of ethylene on adventitious root formation in mung
510 bean hypocotyl cuttings. *Plant Growth Regul.* 36(2), 135-139.
511 doi.org/10.1023/A:1015051725089
- 512 Pitts RJ, Cernac A, Estelle M (1998) Auxin and ethylene promote root hair elongation in
513 *Arabidopsis*. *Plant J*, 16(5), 553-560. doi:10.1046/j.1365-313x.1998.00321.x
- 514 Riov J, Yang SF (1989) Ethylene and auxin-ethylene interaction in adventitious root formation in
515 mung bean (*Vigna radiata*) cuttings. *J Plant Growth Regul*, 8(2), 131.
516 doi:10.1007/BF02025280
- 517 Shingakiwells RN, Huang S, Taylor NL, Carroll AJ, Zhou W, Millar AH (2011) Differential
518 molecular responses of rice and wheat coleoptiles to anoxia reveal novel metabolic
519 adaptations in amino acid metabolism for tissue tolerance. *Plant Physiol.* 156, 1706-1724.
520 doi: 10.4161/psb.6.10.17107
- 521 Shinohara T, Martin EA, Leskovar DI (2017) Ethylene regulators influence germination and root

- growth of globe artichoke seedlings exposed to heat stress conditions. *Seed Sci Technol*, 45(1), 167-178. doi:10.15258/sst.2017.45.1.07
- Simkin AJ, Lopez-Calcagno PE, Davey PA, Headland LR, Lawson T (2017) Simultaneous stimulation of the SBPase, FBP aldolase and the photorespiratory GDC-H protein increases CO₂ assimilation, vegetative biomass and seed yield in Arabidopsis. *Plant Biotechnol J*. 15, 805-816. doi: 10.1111/pbi.12676
- Su NN, Wu Q, Liu YY, Cai JT, Shen WB, Xia K, Cui J (2014) Hydrogen-rich water reestablishes ROS homeostasis but exerts differential effects on anthocyanin synthesis in two varieties of radish sprouts under uv-a irradiation. *J Agr Food Chem*. 62, 6454-6462. doi: 10.1021/jf5019593
- Sugihara K, Hanagata N, Dubinsky Z, Baba S, Karube I (2000) Molecular characterization of cDNA encoding oxygen evolving enhancer protein 1 increased by salt treatment in the mangrove *Bruguiera gymnorhiza*. *Plant and cell physiol*, 41(11), 1279-1285. doi:10.1093/pcp/pcd061
- Sun H, Liu FB, Sun LW, Liu JZ, Wang MY, Chen XN, Xu XH, Ma R, Feng K, Jiang R (2016) Proteomic analysis of differences in amino acid metabolism between wild and cultivated *Panax ginseng*. *J Ginseng Res*. 40, 113-120. doi: 10.1016/j.jgr.2015.06.001
- Torres R, Valentines MC, Usall J, Viñas I, Larrigaudiere C (2003) Possible involvement of hydrogen peroxide in the development of resistance mechanisms in 'Golden Delicious' apple fruit. *Postharvest Biol Tec*. 27, 235-242. doi: 10.1016/S0925-5214(02)00110-2
- Wang J, Pan R (2006) Effect of ethylene on adventitious root formation. In *Ethylene Action in Plants* (pp. 69-79). Springer, Berlin, Heidelberg. doi: 10.1007/978-3-540-32846-9_4
- Wilkinson B, Gilbert HF (2004) Protein disulfide isomerase. *BBA-Proteins Proteom*. 1669,5-44. doi: 10.1016/j.bbapap.2004.02.017
- Wu GX, Wang G, Ji J, Gao HL, Guan WZ, Wu J, Guan CF, Wang YR (2014) Cloning of a cytosolic ascorbate peroxidase gene from *Lycium chinense* Mill and enhanced salt tolerance by overexpressing in tobacco. *Gene* 543, 85-92. doi: 10.1016/j.gene.2014.03.061
- Wu Q, Su, NN, Cai JT, Shen ZG, Cui J (2015) Hydrogen-rich water enhances cadmium tolerance in Chinese cabbage by reducing cadmium uptake and increasing antioxidant capacities. *J Plant Physiol*. 175, 174-182. doi: 10.1016/j.jplph.2014.09.017
- Xie YJ, Mao Y, Zhang W, Lai DW, Wang Q, Shen, WB (2014) Reactive Oxygen species-dependent nitric oxide production contributes to hydrogen-promoted stomatal closure in Arabidopsis. *Plant Physiol*. 165, 759-773. doi: 10.1104/pp.114.237925
- Xu DQ, Gifford RM, Chow WS (1994) Photosynthetic acclimation in pea and soybean to high atmospheric CO₂ partial pressure. *Plant Physiol*. 106, 661-671. doi:10.1104/pp.106.2.643
- Xu XT, Jin X, Liao WB, Mohammed MD, Li XP, Wang M, Niu LJ, Ren PJ, Zhu YC (2017) Nitric oxide is involved in ethylene-induced adventitious root development in cucumber (*Cucumis sativus* L.) explants. *Sci Hortic-Amsterdam*. 215, 65-71. doi.org/10.1016/j.scienta.2016.12.006

- 561 Xu XW, Ji J, Ma XT, Xu Q, Qi XH, Chen XH (2016) Cloning and expression analysis of
562 *Cucumis sativus* calcium-dependent protein kinase 5 gene (*CsCDPK5*) under waterlogging
563 stress. *Acta Hortic.* 43, 704-714. Doi:10.16420/j.issn.0513-353x.2015-0851
- 564 Xuan W, Zhu FY, Xu S, Huang BK, Ling TF, Qi JY, Ye MB, Shen WB (2008) The heme
565 oxygenase/carbon monoxide system is involved in the auxin-induced cucumber adventitious
566 rooting process. *Plant Physiol.* 148, 881-893. doi:10.1104/pp.108.125567
- 567 Yabuta Y, Tamoi M, Yamamoto K, Tomizawa K, Yokota A, Shigeoka S (2008) Molecular
568 designing of photosynthesis-elevated chloroplasts for mass accumulation of a foreign
569 protein. *Plant Cell Physiol.* 49, 375-385. doi: 10.1093/pcp/pcn014
- 570 Zeng JQ, Ye ZH, Su XJ (2014) Progress in the study of biological effects of hydrogen on higher
571 plants and its promising application in agriculture. *Med Gas Res.* 4, 15. doi: 10.1186/2045-
572 9912-4-15
- 573 Zhang D, Ren L, Yue JH, Wang L, Zhuo LH, Hen XH (2013) A comprehensive analysis of
574 flowering transition in *Agapanthus praecox* ssp. *orientalis* (Leighton) Leighton by using
575 transcriptomic and proteomic techniques. *J Proteomics.* 80, 1-25. doi:
576 10.1016/j.jprot.2012.12.028
- 577 Zhang S, Zhang LL, Zhou QY (2015) Comparative proteomic analysis of tetraploid black locust
578 (*Robinia pseudoacacia* L.) cuttings in different phases of adventitious root development.
579 *Trees.* 29, 367-38. doi: 10.1007/s00468-014-1116-9
- 580 Zhu YC, Liao WB (2017) The metabolic constituent and rooting-related enzymes responses of
581 marigold explants to hydrogen gas during adventitious root development. *Theor Exp Plant*
582 *Phys.* 29, 77-85. doi: 10.1007/s40626-017-0085-y
- 583 Zhu YC, Liao WB, Niu LJ, Wang M (2016) Nitric oxide is involved in hydrogen gas-induced
584 cell cycle activation during adventitious root formation in cucumber. *BMC Plant Biol.* 16,
585 146. doi: 10.1186/s12870-016-0834-0

Table 1(on next page)

List of the genes whose transcription profile was evaluated by RT-PCR

Table 1 List of the genes whose transcription profile was evaluated by RT-PCR

Gene name	NCBI accession number	primer	5'-3' primer sequence
CsACS3	AB006805.1	F	5'-CCTTGCAGAGGCTGGCGATG-3'
		R	5'-GGTGACTTGGAAGCCGTTGGAG-3'
CsACO1	AB006806.1	F	5'-AGGTAGGTGGCCTGCAACTCC-3'
		R	5'-CTCCGAGGTTGACGACAATGGC-3'
Rubisco	NP_198657.1	F	5'-GAGATTGAGGAGGCTAAGAAGGAA-3'
		R	5'-GGGCTTGTTAGGCGATGAAAC -3'
SBPase	NP_001267658.1	F	5'-GAGTTCGTTATTTGGGGAGTCATT -3'
		R	5'-TTATCAGGGGTTGCTTTGGTG -3'
TDH	XM_004143321.2	F	5'-CCATTCAACTTTCCAACAGAAC -3'
		R	5'- CGAGCCATCAACAACAGCA-3'
CAPX	NM_001280706	F	5'-TTGGCTGGTGTGTTGCTGT -3'
		R	5'-GGCTCGGGTTTGTCTCTCT -3'
PDI	XM_004149750.2	F	5'- TGAGTTTTACGCCCCCTTGGT-3'
		R	5'-TCTCTGTTTGACTCCTCGTTGG -3'
OEE1	XM-004141898.2	F	5'-TTGAAGTTGGTGCTGATGGTT-3'
		R	5'- GGTGAAGAGGAACGGGACA-3
Actin	DQ115883.1	F	5'-TGGACTCTGGTGATGGTGTTA-3'
		R	5'-CAATGAGGGATGGCTGGAAAA-3'

Table 2(on next page)

Identification and analysis of proteins differentially expressed in response to ETH inhibitor on H₂-induced adventitious root development in cucumber explants

Table 2 Identification and analysis of proteins differentially expressed in response to ETH inhibitor on H₂-induced adventitious root development in cucumber explants

Spot No. ^a	Identified protein ^b	Species	Score ^c	NCBI accession Number	MW ^d	Pi ^e	Peptides Count ^f	Up/Down ^g
K9/1628	Glutamine synthetase	<i>Cucumis sativus</i>	406	KGN57792.1	39251.8	5.82	13	↓
K10/2129	ribulose biphosphate carboxylase/oxygenase precursor peptide	<i>Cucumis sativus</i>	78	AAA33131.1	21049.4	7.55	12	↑
K11/1937	Unknow protein	<i>Cucumis sativus</i>	234	KGN44928.1	22556.6	4.45	13	↓
K12/1908	Cytosolic ascorbate peroxidase	<i>Cucumis sativus</i>	595	KGN65655.1	27377.8	5.43	17	↑
K13/1561	Sedoheptulose-1,7-bisphosphatase	<i>Cucumis sativus</i>	534	KGN50632.1	42075.4	5.96	22	↑
K14/1799	Eukaryotic translation elongation factor 1 delta isoform X1	<i>Cucumis sativus</i>	417	XP_011652060.1	24670.3	4.45	15	↓
K15/1817	Oxygen-evolving enhancer protein 1	<i>Cucumis sativus</i>	905	KGN48464.1	34938.8	6.24	24	↓
K16/2139	PREDICTED:11S globulin seed storage protein 2-like	<i>Cucumis sativus</i>	458	XP_011652795.1	54382	5.71	11	↓
K17/2062	Cytochrome b6-f complex iron-sulfur subunit	<i>Cucumis sativus</i>	112	KGN43571.1	24255.2	8.45	9	↓
K18/1169	Chloroplast transketolase	<i>Cucumis sativus</i>	712	KGN56609.1	80569.6	6	27	↓
K19/2156	Ribulose biphosphate carboxylase small chain	<i>Cucumis sativus</i>	68	KGN52085.1	20685.2	8.24	11	↓
K20/1284	ATPase alpha subunit (chloroplast)	<i>Cucumis sativus</i>	385	AAZ94637.1	55348	5.13	24	↑
K21/2064	ATPase alpha subunit (chloroplast)	<i>Cucumis sativus</i>	246	AAZ94637.1	55348	5.13	20	↓
K22/361	26S protease regulatory subunit 6A homolog	<i>Cucumis sativus</i>	230	XP_004135596.1	38614.9	5.16	21	↓
K23/748	Oxygen-evolving enhancer protein 1	<i>Cucumis sativus</i>	752	KGN48464.1	34938.8	6.24	20	↓
K24/533	Mg-protoporphyrin IX chelatase	<i>Cucumis sativus</i>	236	KGN49283.1	45728	5.72	20	↓
L1/203	Protein disulfide-isomerase	<i>Cucumis sativus</i>	83	KGN47715.1	57045.6	4.88	12	↑
L2/230	Threonine dehydratase	<i>Cucumis sativus</i>	620	KGN48214.1	67198.9	6.22	25	↑
L3/1196	PSII reaction center subunit V (chloroplast)	<i>Cucumis sativus</i>	103	AAZ94668.1	9380.7	4.83	4	↓
L4/858	Cytosolic ascorbate peroxidase	<i>Cucumis sativus</i>	716	KGN65655.1	27377.8	5.43	15	↑
L6/656	Proteasome subunit alpha type	<i>Cucumis sativus</i>	466	KGN62618.1	30861.4	4.98	9	↓
L7/1009	Unknow	<i>Cucumis sativus</i>	412	KGN57117.1	18646.5	4.56	9	↓
L8/158	Malic enzyme	<i>Cucumis sativus</i>	496	KGN66170.1	65093.8	5.72	23	↑
L9/975	Chlorophyll a-b binding protein,	<i>Cucumis sativus</i>	270	KGN51208.1	26517.6	5.84	7	↑

	chloroplastic							
L10/1116	60S acidic ribosomal protein P1	<i>Cucumis sativus</i>	355	KG556349.1	11414.7	4.34	3	↑
L11/747	Cysteine protease	<i>Cucumis sativus</i>	114	KG62647.1	40614.9	5.2	8	↓
L12/200	Protein disulfide-isomerase	<i>Cucumis sativus</i>	90	KG47715.1	57045.6	4.88	18	↓
L13/527	Mg-protoporphyrin IX chelatase	<i>Cucumis sativus</i>	200	KG49283.1	45728	5.72	19	↓
L14/1132	Ribulose biphosphate carboxylase small chain	<i>Cucumis sativus</i>	100	KG52085.1	20685.2	8.24	11	↑
L15/502	Unknow	<i>Cucumis sativus</i>	312	KG57401.1	31417.5	4.82	5	↓
L16/626	Sedoheptulose-1,7- biphosphatase	<i>Cucumis sativus</i>	546	KG50632.1	42075.4	5.96	18	↑
L17/896	PREDICTED: 29 kDa ribonucleoprotein, chloroplastic	<i>Cucumis sativus</i>	298	XP_004137828.1	30479.5	5.84	7	↓
L18/103	Chloroplast HSP70	<i>Cucumis sativus</i>	412	KG61439.1	75350	5.18	25	↓
L19/447	30S ribosomal protein S1, chloroplastic	<i>Cucumis sativus</i>	496	XP_004147619.1	45304.5	5.34	18	↓
L20/1129	PREDICTED: 60S acidic ribosomal protein P2-4	<i>Cucumis sativus</i>	93	XP_004150488.1	11419.9	4.53	8	↓
L21/982	PREDICTED: 11S globulin subunit beta	<i>Cucumis sativus</i>	479	XP_011651441.1	57575.8	7.21	15	↓
L22/1140	ribulose-1,5-bisphosphate carboxylase small subunit	<i>Cucumis sativus</i>	113	CCF55356.1	20713.2	8.24	15	↑
L23/732	PREDICTED: 14-3-3-like protein D	<i>Cucumis sativus</i>	120	XP_004136830.1	29379.5	4.76	10	↓
M15/139	PREDICTED: ruBisCO large subunit-binding protein subunit alpha	<i>Cucumis sativus</i>	401	XP_004145754.1	61399.9	5.06	26	↓
M17/239	Oxygen-evolving enhancer protein 1	<i>Cucumis sativus</i>	216	KG48464.1	34938.8	6.24	19	
M18/1018	PREDICTED: 60S acidic ribosomal protein P1	<i>Cucumis sativus</i>	170	KG556349.1	11414.7	4.34	2	↓
M19/1030	Cytosolic ascorbate peroxidase	<i>Cucumis sativus</i>	407	KG65655.1	27377.8	5.43	17	↓
M20/340	ribulose-1,5-bisphosphate carboxylase small subunit	<i>Cucumis sativus</i>	137	CCF55356.1	20713.2	8.24	14	↓
M21/162	Threonine dehydratase	<i>Cucumis sativus</i>	206	KG48214.1	67198.9	6.22	22	↓
M23/462	Sedoheptulose-1,7- biphosphatase	<i>Cucumis sativus</i>	250	KG50632.1	42075.4	5.96	18	↓
M24/354	Beta-form rubisco activase	<i>Cucumis sativus</i>	241	KG50568.1	48292.6	8.19	19	↓
N1/351	Unknow	<i>Cucumis sativus</i>	238	KG59544.1	36680	4.7	23	↓
N2/117	Protein disulfide-isomerase	<i>Cucumis sativus</i>	62	KG47715.1	57045.6	4.88	16	↓

Spots K9/1628 to K21/2064 were the proteins in ETH treatment; K22/361 to L23/732 were the proteins in ETH treatment and the control; M15/139 to N2/117 were the proteins in HRW+AVG treatment.

- 5 ^a Spot numbers are arbitrary as assigned by the software of PD-Quest 8.0.
- 6 ^b The name and functional categories of the proteins using MALDI TOF-TOF MS.
- 7 ^c The Mascot score obtained after searching against the NCBI nr database.
- 8 ^{d, e} Theoretical molecular mass (MV) and isoelectric point (PI) of the identified protein.
- 9 ^f Number of peptides sequenced.
- 10 ^g “↑” represents up-regulated expression, “↓” represents down-regulated expression.

Table 3(on next page)

Analysis of differential protein expression during H₂, ETH and AVG-induced adventitious root development

Table 3 Analysis of differential protein expression during H₂, ETH and AVG-induced adventitious root development

Protein name	Functional category	Control	H ₂	ETH	H ₂ +AVG
ribulose-1,5-bisphosphate carboxylase small subunit	Photosynthesis	—	↑	↑	↓
Sedoheptulose-1,7-bisphosphatase	photosynthesis	—	↑	↑	↓
Threonine dehydratase	amino and metabolism	—	↑	—	↓
Cytosolic ascorbate peroxidase	stress response	—	↑	↑	↓
Protein disulfide-isomerase	Protein folding, modification and degradation	—	↑	—	↓
Oxygen-evolving enhancer protein 1	photosynthesis	—	↓	↓	↑

“↑” represents up-regulated expression, “↓” represents down-regulated expression.

Figure 1

Effects of different concentrations of HRW on adventitious root development.

The primary root system was removed from hypocotyls of 7-day-old germinated cucumber. Explants were incubated with distilled water or different concentrations of HRW and indicated for 7 days. The number (**A**) of adventitious roots per explant were expressed as mean \pm SE (n = 20 explants from each of four independent experiments). Bars with different lowercase letters were significantly different (Duncan's multiple range test, $P < 0.05$). Photographs (**B-F**) show hypocotyl explants after 7 days of the treatments indicated.

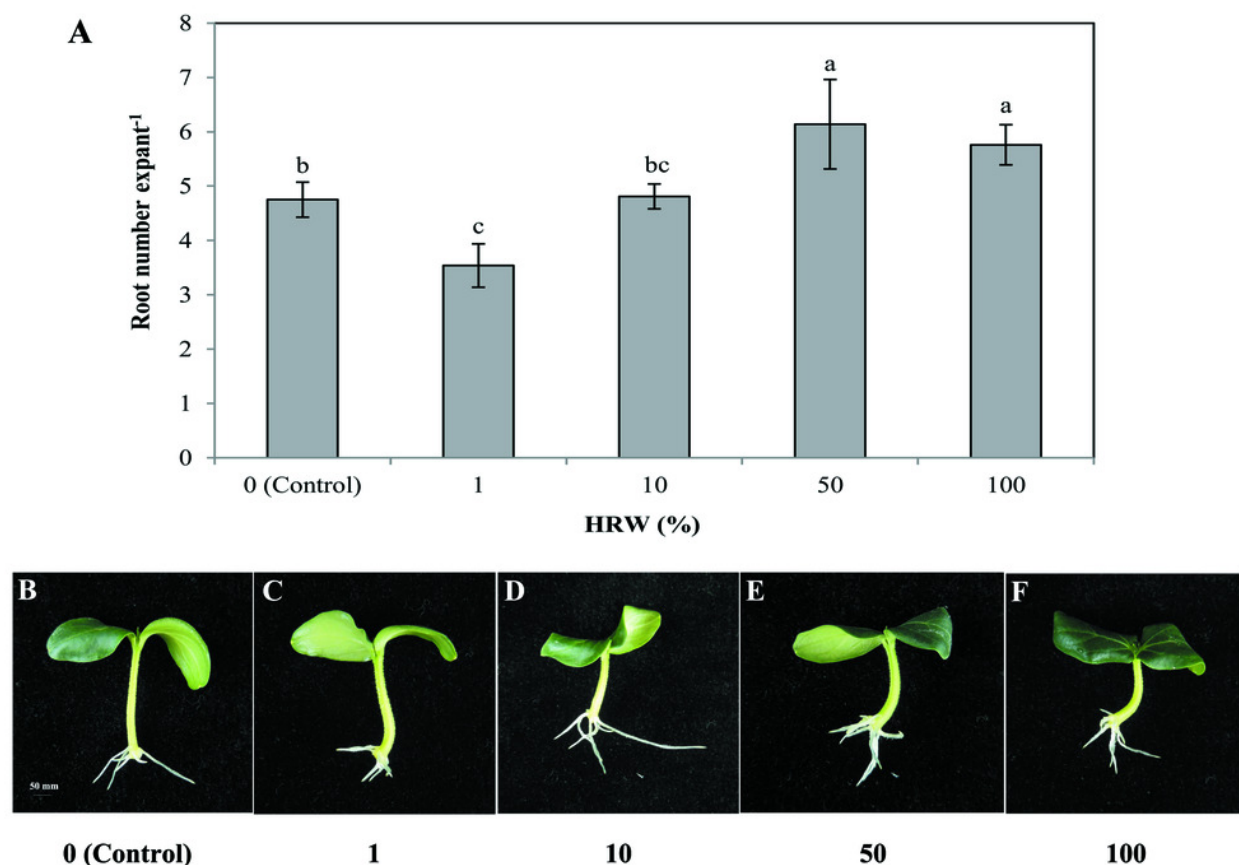


Figure 2

Effects of different concentrations of ethephon on adventitious root development.

The primary root system was removed from hypocotyls of 7-day-old germinated cucumber. Explants were incubated with distilled water or different concentrations of ethephon and indicated for 7 days. The number (**A**) of adventitious roots per explant were expressed as mean \pm SE (n = 20 explants from each of four independent experiments). Bars with different lowercase letters were significantly different (Duncan's multiple range test, $P < 0.05$). Photographs (**B-G**) show hypocotyl explants after 7 days of the treatments indicated.

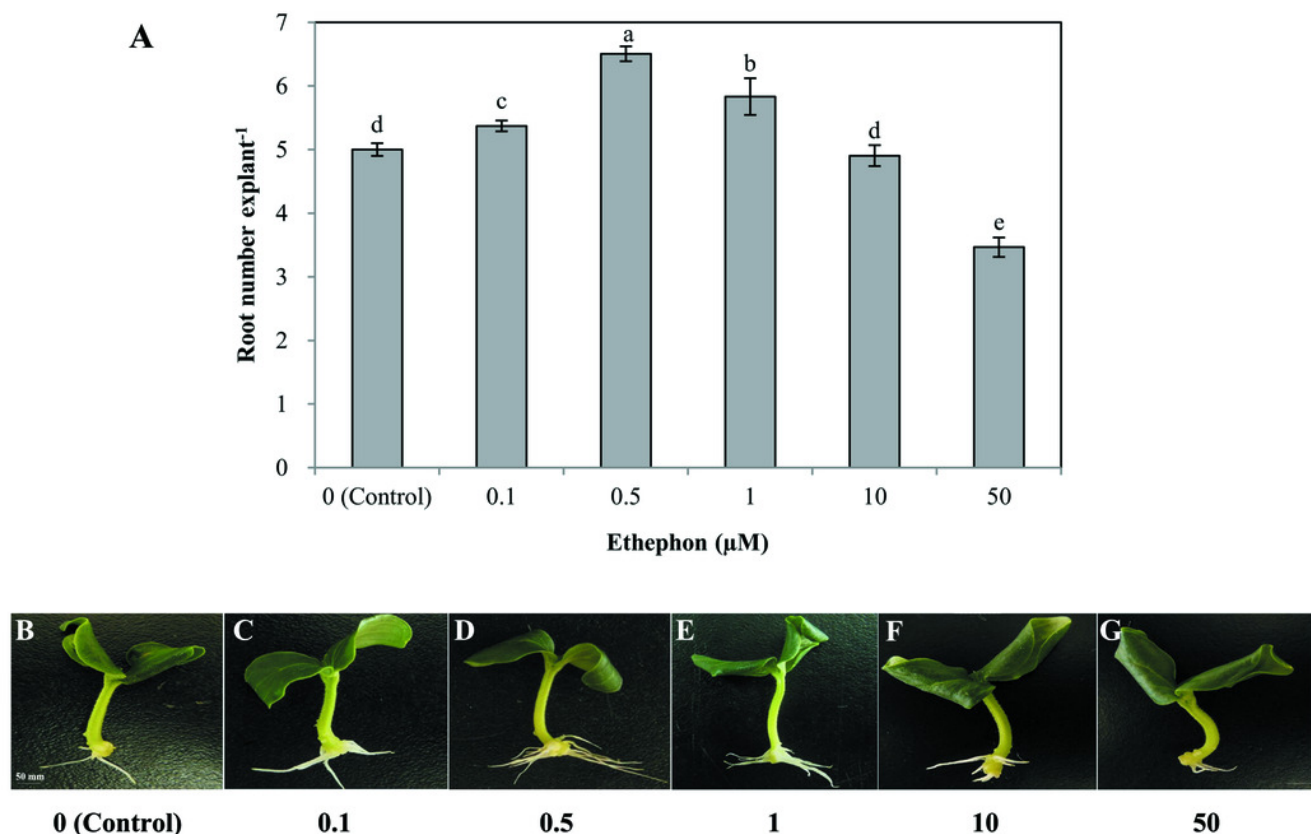


Figure 3

Effects ETH inhibitor on H₂-induced adventitious root development.

The primary root system was removed from hypocotyls of 7-day-old germinated cucumber. Explants of cucumber were incubated with 0.5 μ M ethephon, 50% HRW, 50% HRW + 0.5 μ M ethephon, 50% HRW + 1 μ M AVG, 50% HRW+ 0.1 μ M AgNO₃/NaNO₃ and indicated for 7 days. The number (**A**) of adventitious roots per explant were expressed as mean \pm SE (n = 20 explants from each of four independent experiments). Bars with different lowercase letters were significantly different (Duncan's multiple range test, $P < 0.05$). Photographs (**B-G**) show hypocotyl explants after 7 days of the treatments indicated.

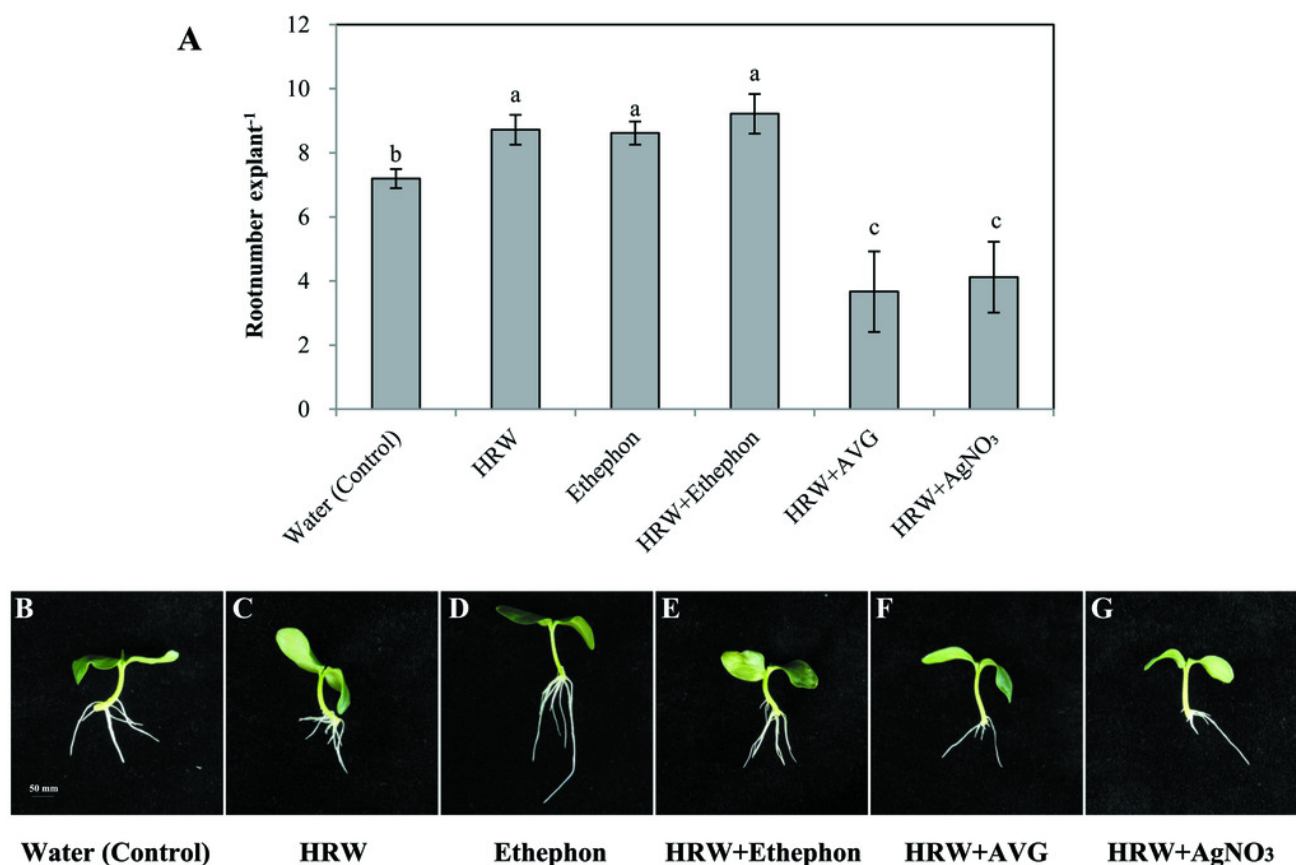


Figure 4

The effect of HRW on the ETH production (A) and on the expression level (B) of two ETH-related genes in cucumber explant.

The values (means \pm SE) are the average of three independent experiments. Bars with an asterisk presents significant ($P < 0.05$), and two asterisks presents very significant ($P < 0.01$).

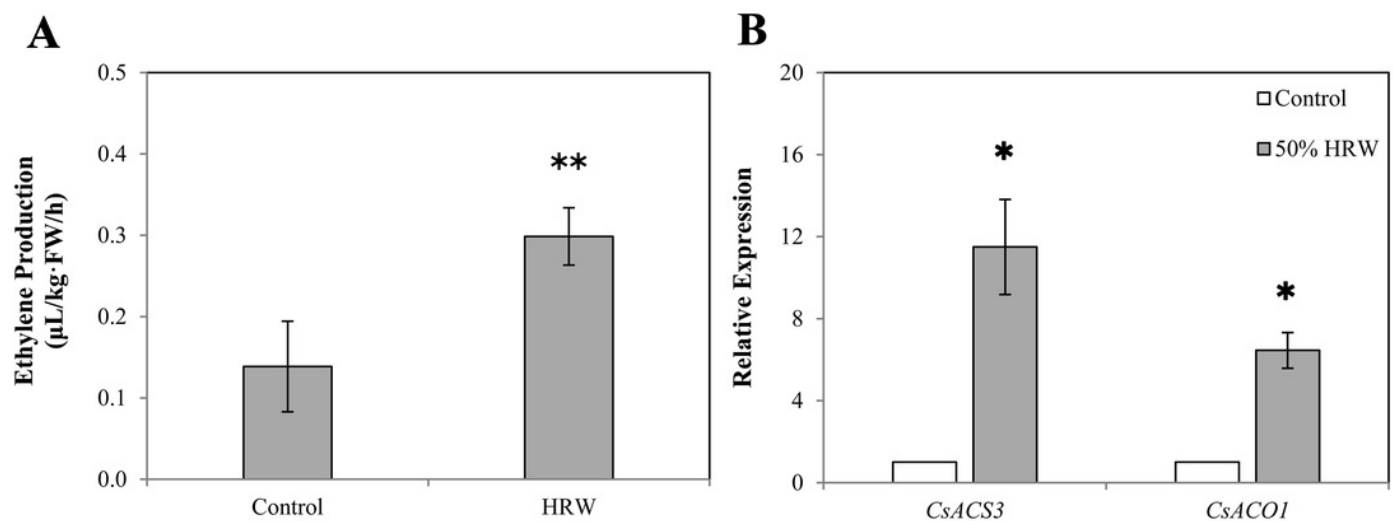


Figure 6

The functional classification and distribution of all 41 identified proteins.

Unknown proteins include those whose functions have not been described.

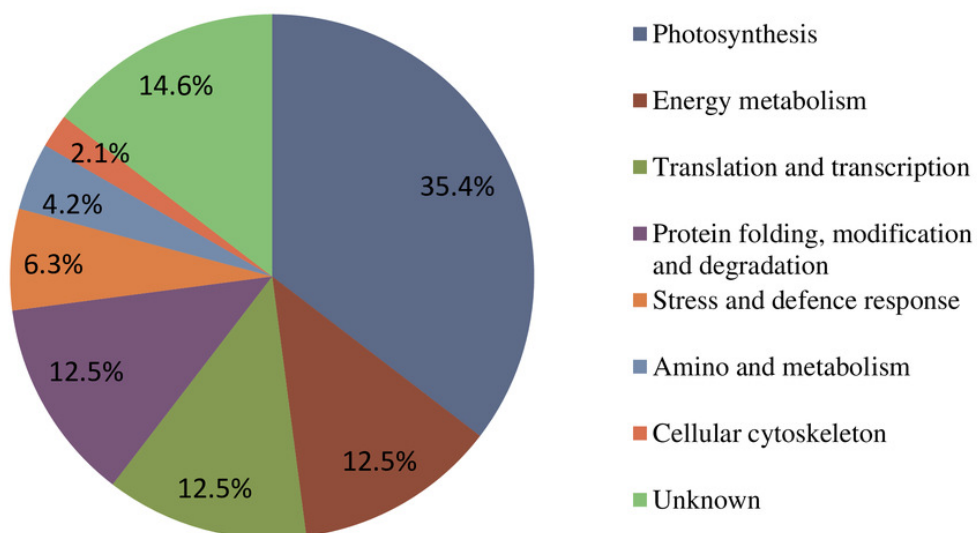


Figure 7

The gene ontology (GO) analysis of the identified proteins.

Information of number and percentage of involved proteins in a term are shown in left and right y-axis.

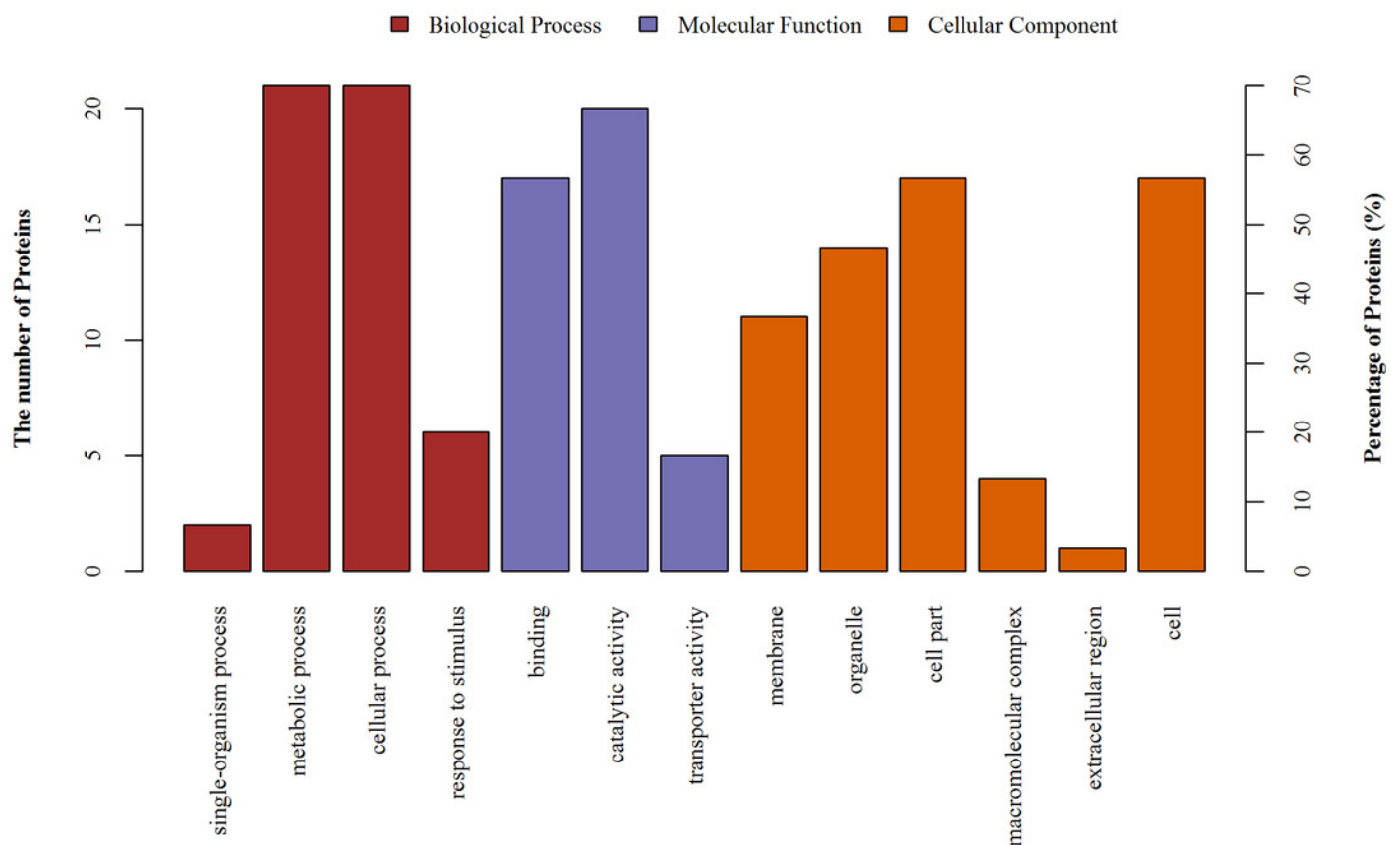


Figure 8

The effect of ETH and HRW on the expression levels of *rbcS* (A), *SBPase* (B), *TDH* (C), *OEE1* (D), *CAPX* (E) and *PDI* (F).

The values (means \pm SE) are the average of three independent experiments. Bars with different lowercase letters were significantly different by Duncan's multiple range test ($P < 0.05$).

